Pflugers Arch - Eur J Physiol (2016) 468:269–278
DOI 10.1007/s00424-015-1738-9

MUSCLE PHYSIOLOGY

Unexpected dependence of RyR1 splice variant expression in human lower limb muscles on fiber-type composition

Hermia Willemse[1] · **Angelo Theodoratos**[1] · **Paul N. Smith**[2] · **Angela F. Dulhunty**[1]

Received: 9 July 2015 / Revised: 14 September 2015 / Accepted: 29 September 2015 / Published online: 6 October 2015

Abstract The skeletal muscle ryanodine receptor Ca^{2+} release channel (RyR1), essential for excitation-contraction (EC) coupling, demonstrates a known developmentally regulated alternative splicing in the ASI region. We now find unexpectedly that the expression of the splice variants is closely related to fiber type in adult human lower limb muscles. We examined the distribution of myosin heavy chain isoforms and ASI splice variants in gluteus minimus, gluteus medius and vastus medialis from patients aged 45 to 85 years. There was a strong positive correlation between ASI(+)RyR1 and the percentage of type 2 fibers in the muscles (r=0.725), and a correspondingly strong negative correlation between the percentages of ASI(+)RyR1 and percentage of type 1 fibers. When the type 2 fiber data were separated into type 2X and type 2A, the correlation with ASI(+)RyR1 was stronger in type 2X fibers (r=0.781) than in type 2A fibers (r=0.461). There was no significant correlation between age and either fiber-type composition or ASI(+)RyR1/ASI(−)RyR1 ratio. The results suggest that the reduced expression of ASI(−)RyR1 during development may reflect a reduction in type 1 fibers during development. Preferential expression of ASI(−) RyR1, having a higher gain of in Ca^{2+} release during EC coupling than ASI(+)RyR1, may compensate for the reduced terminal cisternae volume, fewer junctional contacts and reduced charge movement in type 1 fibers.

Keywords Human skeletal muscle · Ryanodine receptor · ASI splice variants · Fiber types · Aging

Electronic supplementary material The online version of this article (doi:10.1007/s00424-015-1738-9) contains supplementary material, which is available to authorized users.

✉ Angela F. Dulhunty
angela.dulhunty@anu.edu.au

Hermia Willemse
Hermia.Willemse@canberra.edu.au

Angelo Theodoratos
angelo.theodoratos@anu.edu.au

Paul N. Smith
psmith@orthoact.com.au

[1] John Curtin School of Medical Research, Australian National University, Acton, ACT 2600, Australia

[2] Trauma and Orthopaedic Research Unit, Canberra Hospital, Building 6, Level 1, P.O. Box 11, Woden, ACT 2606, Australia

Background

In this study, we have examined the fiber-type distribution of alternatively spliced region I (ASI) variants of the skeletal muscle ryanodine receptor (RyR1) in human lower limb muscles. RyR1 is an essential component of excitation-contraction (EC) coupling in skeletal muscle. RyR1 is activated to release Ca^{2+} from the sarcoplasmic reticulum (SR), through a physical interaction with the transverse (t-) tubular voltage sensor, the L-type voltage gated Ca^{2+} channel ($Ca_V1.1$), also known as the dihydropyridine receptor (DHPR). The resultant rise in cytoplasmic Ca^{2+} facilitates muscle contraction. Mammalian fast- and slow-twitch skeletal muscle contains a variety of fiber types which have been extensively reviewed by Schiaffino and Reggiani [32] and which demonstrate significant differences in components of EC coupling [32].

RyR1 is developmentally spliced in two regions, alternatively spliced region I (ASI) and II (ASII) [15, 38]. The ASI region (residues 3481–3485) is located in helix 20 of the Helical Domain 2 (HD2) cytoplasmic region of RyR1, and the ASII region (residues 3865–3870) is located between helix 9 and 10 of the central cytoplasmic domain [36]. The ASI

region is located close to five basic residues 3495–3502 (in helix 21 of the HD2 region [36]) which binds to the beta subunit ($Ca_V\beta_{1a}$) of the DHPR [6]. Both ASI and 3495–3502 [6, 18] affect the gain of EC coupling. The ASI region contains 15 bp that are included in ASI(+)RyR1 transcript or excluded in the ASI(−)RyR1 transcript, resulting in the presence or absence of five amino acid residues Ala^{3481}-Gln^{3485} in rabbit RyR1 [15]. Analysis of splicing patterns in the hind limb muscles of mice indicated that ASI(−)RyR1 alone is detected in embryonic muscle and dominates in juvenile muscle, with the proportion of ASI(+)RyR1 increasing gradually with development [15] to a molar ratio of ~3:1 (ASI(+)/ASI(−)) in adult skeletal muscle.

Kimura et al. [19] investigated RyR1 splicing in patients with myotonic dystrophy type 1 (DM1), a dominantly inherited multi-systemic disorder including skeletal muscle, caused by unstable expansion of CTG trinucleotide repeats in the myotonic dystrophy protein kinase (DMPK) gene [16]. Kimura et al. showed that there is a shift in the ratio of ASI(+)RyR1/ASI(−)RyR1 in adult patients with DM1 to a predominantly juvenile ASI(−)RyR1 type. However, they did not examine fiber-type distributions in these muscles and proposed that RyR1 is one of the aberrantly spliced proteins in patients with DM1, resulting in a predominance of the juvenile isoform ASI(−)RyR1.

We have examined the ASI splicing pattern of RyR1 as well as the distribution of fiber types in gluteus minimus, gluteus medius, and vastus medialis muscles from middle aged to aging patients. It seemed possible that the levels of juvenile RyR1 (ASI(−)RyR1) might be elevated in aging muscle, since a characteristic of aging muscle is the increased muscle fiber denervation and reinnervation [10]. The regenerated fibers do not undergo complete maturation and morphologically resemble myotubes [9] expressing juvenile isoforms of proteins. However, we did not find any correlation between age and RyR1 ASI splice variants, but we made a surprising observation that there is a strong correlation between ASI splice variants and fiber-type distribution, indicating a fiber-type-specific splicing of RyR1 in mammalian skeletal muscle.

Methods

Collection of human muscle

Muscle samples from patients undergoing hip replacements (gluteus minimus and gluteus medius) or knee replacements (vastus medialis) were collected in theatre. Written informed consent was obtained from each patient for donating tissue. Samples were rinsed in phosphate-buffered saline (PBS) containing 2 mM EGTA, excess fat, and connective tissue removed, cut into approximately 80-mg pieces and then immediately snap-frozen in liquid nitrogen and stored at 70 °C until further processing. Ethical approval for the study was obtained from ACT Health Human Research Ethics Committee (ETH.9/07.865) and the ANU Human Ethics Committee (Protocol 2013/307).

Determination of fiber-type distribution

The fiber-type distribution of muscle samples was determined using sodium dodecyl sulfate polyacrylamide gel electrophoresis (SDS-PAGE) to separate the myosin heavy chain (MyHC) isoforms as previously described [25, 34] with the following modifications. Muscle samples were thawed on ice in 1 ml of cold homogenizing buffer (20 mM imidazole pH 7.2, 120 mM KCl, 0.2 mM EDTA-Na_2) with protease inhibitor cocktail (Roche, Switzerland). Muscle was homogenized and the homogenate centrifuged at 11,752×*g* for 20 min at 4 °C. The pellet was resuspended in 100–200 μl resuspending buffer (50 mM Tris-HCl pH 7.4, 150 mM NaCl), adjusted to a final concentration of 0.4 mg/ml and aliquots snap-frozen in liquid nitrogen until further use.

An SDS-PAGE gel was prepared as follows and allowed to polymerize overnight: resolving gel of 8 % polyacrylamide (acrylamide/bis-acrylamide ratio of 99:1) containing 35 % glycerol and stacking gel of 4 % polyacrylamide (acrylamide/bis-acrylamide ratio of 49:1) containing 30 % glycerol. Muscle homogenate samples were mixed with a 3× sample buffer (0.34 M Tris HCl pH 6.8, 60 % glycerol, 6 % SDS, 150 mM DTT, 0.01 % bromophenol blue) and boiled for 2 min. Three micrograms of protein was loaded onto the gel and the gel run for 20 h at 4 °C. The outer buffer dam contained 1× running buffer (50 mM Tris, 75 mM Glycine, 0.05 % SDS), whereas the inner buffer dam contained 8× running buffer (0.4 M Tris, 0.6 M glycine, 0.4 % SDS) containing 0.12 % 2-mercaptoethanol. Gels were stained using a Silver Stain Plus Kit (Bio-Rad Laboratories, USA)) and documented and analyzed by digital imaging using a Gel Doc XR System and Quantity One 1-D analysis Software (Bio-Rad Laboratories, USA)) after drying.

RNA extraction from muscle tissue and cDNA synthesis

Total RNA was extracted from human muscle samples using TRIzol reagent (Invitrogen, Life Technologies, USA) and RNeasy Mini Kit (QIAGEN, Netherlands). The extracted RNA was then treated with the TURBO DNA-free Kit (Ambion, Life Technologies, USA) to remove any DNA contamination. RNA concentration was determined spectrophotometrically.

RNA was converted to cDNA using the SuperScript III Reverse Transcriptase Kit (Invitrogen, Life Technologies, USA) and $Oligo(dT)_{12–18}$ primers (Invitrogen, Life Technologies, USA).

PCR analysis of splice variants

ASI regions were amplified using the KOD Hot Start DNA Polymerase Kit (Novagen, Merck Millipore, Germany) with primers described in [19]. The PCR consisted of 35 cycles with an annealing temperature of 62 °C. PCR products were 69 and 54 bp for ASI(+)RyR1 and ASI(−)RyR1, respectively. The PCR product was separation by electrophoresis on 10 % polyacrylamide gels. Quantitative analysis of amplified products was performed with the Gel Doc XR System and Quantity One 1-D analysis Software (Bio-Rad Laboratories, USA).

Statistical analysis

MyHC bands as well as PCR products were expressed as a percentage of the total MyHC or PCR product present. Statistical significance was assessed using unpaired Student's *t* tests assuming unequal variance ($P<0.05$) and Pearson correlations. Correlations were deemed significant if the correlation coefficient (r) differed significantly from 0 ($P<0.05$).

Results

Human muscle samples were obtained from 38 donors undergoing hip replacement (gluteus minimus and gluteus medius) or knee replacement (vastus medialis) surgery. A list of the age and gender of the donors is given in Table 1.

Fiber-type distribution of muscle samples The myosin heavy chain (MyHC) isoforms were visualized on Silver Stained SDS polyacrylamide gels (Fig. 1a) and the density of each band expressed as a percentage of the total amount of MyHC in the sample, with four repeats of each sample. The average distribution of fiber types in each of the muscles is shown in Fig. 1b. Both gluteus minimus and gluteus medius contained predominantly type 1 fibers with no significant difference in the percentage of type 1 fibers. However, gluteus minimus had significantly more type 2A fibers than gluteus medius. There was, however, no significant difference in type 2X content. Vastus medialis, on the other hand, contained predominantly type 2 fibers, with significantly fewer type 1 fibers than the gluteal muscles and significantly more type 2A and 2X.

When the fiber-type distribution of each muscle type was plotted against the age of the donors, there was no correlation with age in any of the muscles (Fig. 2). Due to the small number of gluteus medius samples (Online resource 1), a correlation between fiber type and age could not be determined.

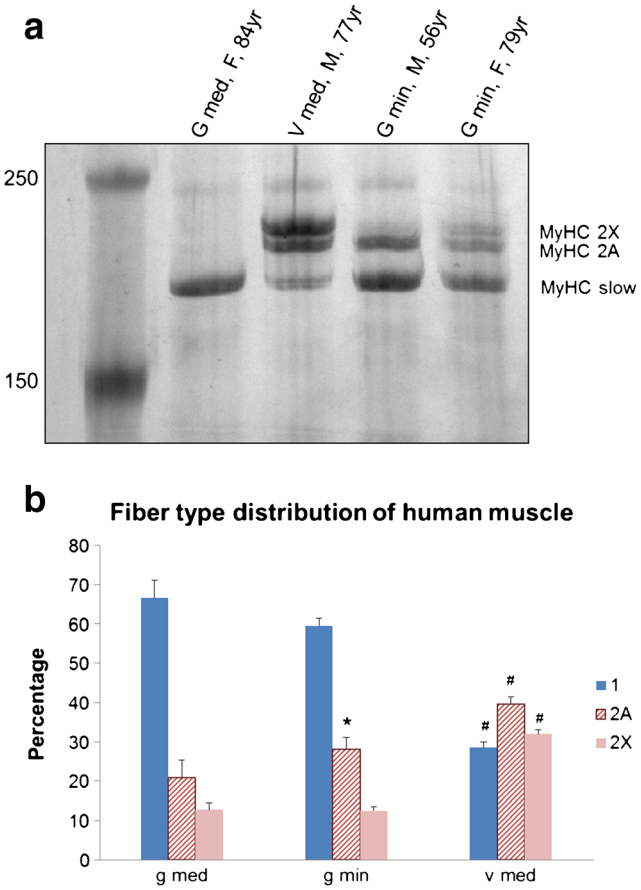

Fig. 1 The fiber-type distribution of each muscle. **a** An example of the silver stained gel used to separate the MyHC isoforms. The *first lane* contains the protein markers corresponding to 250 and 150 kDa. **b** The average percentage of each MyHC isoform indicating the fiber-type distribution for the respective muscles. The fiber-type determination was repeated three to four times for each sample and the average determined for each muscle. *Significantly different from gluteus medius $P<0.05$; #significantly different from gluteus minimus and gluteus medius $P<0.01$

Table 1 Breakdown of human muscle samples from 38 donors indicating the muscle source, gender, and age

Gluteus medius		Gluteus minimus		Vastus medialis	
Female	Male	Female	Male	Female	Male
52	72	51	45	54	59
76		52	47	56	66
84		58	52	57	69
		61	56	62	71
		66	59	64	73
		70	60	64	77
		71	61	74	
		74	69		
		79	70		
		82	72		
		85			

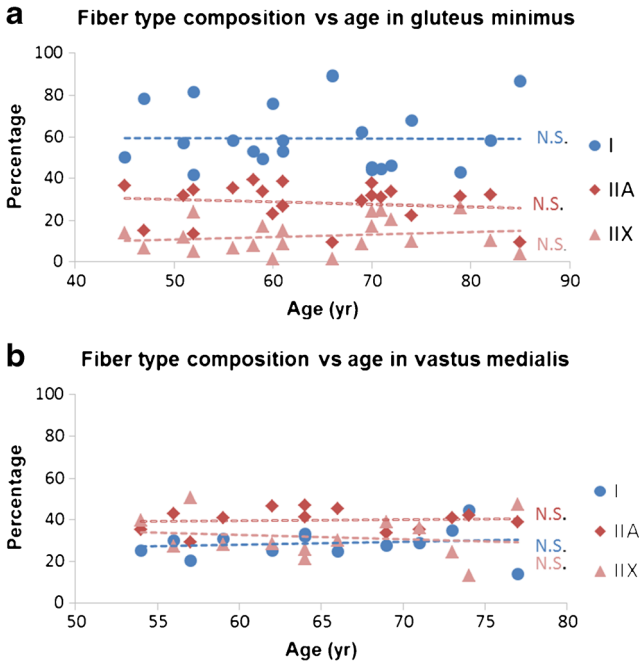

Fig. 2 The fiber-type distribution of each muscle plotted against the age of the respective donors. **a** The fiber-type distribution in gluteus minimus. **b** The fiber-type distribution in vastus medialis. **c** The fiber-type distribution in gluteus medius. *N.S.* no significant correlation, I type 1 fibers, IIA type 2A fibers, IIX type 2X fibers

Splice variant analysis The ratio of RyR1 ASI splice variants was determined for each of the muscle samples. RT-PCR was performed on all samples at the same time in the same apparatus to ensure that the conditions did not vary. Examples of polyacrylamide gels showing the RT-PCR products are shown in Fig. 3a. The density of the RT-PCR bands on the gels was measured and expressed as a percentage of the total RT-PCR product of the RyR1 ASI region present for each sample. The resulting ASI(+)/ASI(−) ratio for each of the 38 samples as well as its corresponding fiber-type distribution is shown in Table 2.

To ensure that the band intensity for each sample was not affected by saturation of the PCR reaction, two representative examples of samples having (a) a high ASI(+)RyR1/ASI(−)RyR1 ratio, (b) equal amounts of ASI(+)RyR1 and ASI(−)RyR1, or (c) a low ASI(+)RyR1/ASI(−)RyR1 ratio were selected and the PCR repeated with 28 cycles, 32 cycles, and 35 cycles for each sample (Fig. 3c). From the results, it is clear that the PCR reaction was not saturated and the results obtained for all samples with 35 cycles provide a true reflection of ASI(+)/ASI(−) ratio.

RyR1 ASI splice variant levels vs. age The percentage of ASI(+)RyR1 and ASI(−)RyR1 transcript was plotted against the ages of the donors and the Pearson correlation coefficient used to determine correlation (Fig. 4). Data from the three muscles is included in each graph. Gluteus minimus and vastus medialis are shown separately in Online resource 2. In contrast to our starting hypothesis, there was no significant decline in the percentage of ASI(+)RyR1 transcript in older patients (Fig. 4a) and, hence, also no increase in the percentage ASI(−)RyR1 transcript in older patients (Fig. 4b).

RyR1 ASI splice variant levels vs. muscle and fiber-type distribution Remarkably, while investigating a potential relationship between fiber type and age, we discovered a significant difference ($P<0.01$) between the percentage of ASI(+) in vastus medialis and both gluteus medius and gluteus minimus (Fig. 5). There was significantly more ASI(+) RyR1 expressed in vastus medialis, which has a significantly greater number of type 2A and 2X fibers, as shown in Fig. 1b (above).

The fiber-type dependence of ASI splice variant expression is further illustrated by a positive correlation between the combined fast, type 2 fiber content and the content of ASI(+)RyR1 transcript (Fig. 6a, $r=0.725$, $r^2=0.525$). An even stronger positive correlation ($r=0.781$, $r^2=0.610$) was found between the percentage ASI(+)RyR1 transcript and the content of the fastest oxidative type 2X fibers (Fig. 6b). The correlation between the percentage of ASI(+)RyR1 transcript and the content of type 2A fiber was also significant ($r=0.461$, $r^2=0.212$, Fig. 6c). Conversely, there was a strong negative correlation between the percentage of ASI(+)RyR1 transcript and content of slow type 1 fibers (Fig. 7a) and a correspondingly strong positive correlation between ASI(−)RyR1 and the type 1 fiber content (Fig. 7b). Therefore, we report novel data (Figs. 5, 6, and 7) illustrating a significant and previously unsuspected fiber-type dependence of expression of the ASI spice variants of RyR1.

Discussion

The novel results reported here provide compelling evidence that expression of ASI splice variants of RyR1 is fiber-type-dependent in human lower limb muscle, in addition to the known role in development [15], with the ASI(+) splice variant increasing proportionally with the fastest glycolytic fibers. A fiber-type dependence of RyR1 isoforms has not previously been described in mammalian muscle. We suggest that the relative amounts of ASI isoform present in the muscle may have functional consequences for the gain of EC coupling in type 1 and type 2 fibers in humans.

RyR1 ASI splice variant levels vs. muscle and fiber-type distribution Zorzato et al. [38] showed that two splice variants of RyR1 (corresponding to the ASI variants described later by Futatsugi et al. [15]) are present in slow- and fast-twitch muscle, but they did not measure the relative amounts of the transcripts. In mouse hind limb muscle containing mostly fast-twitch fibers, Futatsugi et al. [5] report an adult ASI

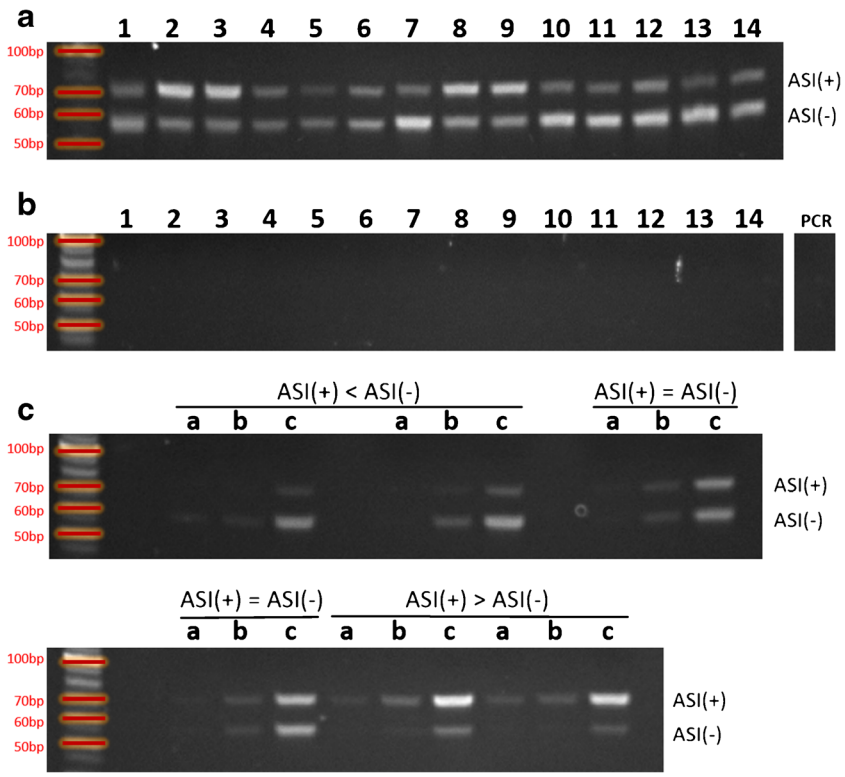

Fig. 3 Examples of the RT-PCR product in the splice variant analysis of the RyR1 ASI region. **a** RT-PCR product from 14 of the human muscle donor samples. The ASI(+)RyR1 and ASI(−)RyR1 PCR products are 60 and 54 bp, respectively. The *lanes* contain the following samples: gluteus minimus (g min), F, 51 years (***1***); vastus medialis (v med), F, 54 years (***2***); v med, F, 71 years (***3***); gluteus medius (g med), F, 76 years (***4***); g min, M, 60 years (***5***); g min, F, 74 years (***6***); g min, F, 58 years (***7***); v med, M, 50 years (***8***); v med, M, 73 years (***9***); g min, F, 52 years (***10***); g med, F, 52 years (***11***); g min, F, 61 years (***12***); g min F, 66 years (***13***); g min, F, 79 years (***14***). **b** Negative controls of the RT-PCR reaction for each of the samples in **a** containing no reverse transcriptase enzyme, PCR—negative control for the PCR reaction containing no cDNA template. **c** Control experiment to show that PCR reaction was not saturated at 35 cycles and that differences seen in band density are a true reflection of amounts of ASI(+)RyR1 and ASI(−)RyR1 mRNA in the muscle. Representative samples with ASI(+) product less that ASI(−), ASI(+) product equal to ASI(−) product, and ASI(+) product more than ASI(−) product were selected and **a** PCR of 28 cycles, **b** PCR of 32 cycles, and **c** PCR of 35 cycles performed

splice variant ratio (ASI(+)RyR1/ASI(−)RyR1) of 3:1 [15]. In light of our findings, it is possible that the predominance of ASI(+)RyR1 may be due to the predominance of type 2 fibers in these muscles. During muscle development in mice, fast-twitch MyHC isoforms appear only during the first week after birth. Earlier, the developmental (embryonic MyHC and neonatal MyHC) and slow MyHC isoforms are exclusively expressed [1]. The time frames for the appearance of the fast MyHC isoforms and the ASI(+)RyR1 splice variant coincide suggesting an interdependence [1, 15]. Although this would have to be confirmed by simultaneous measurement of ASI splicing and MyHC isoforms during development, the simultaneous appearance of ASI(+)RyR1 and the fast MyHC isoforms supports our finding that the ASI splice variant levels are fiber-type-dependent.

ASI splice variant analysis in rectus abdominus muscle from normal and DM1 patients has been reported, without an examination of fiber-type distribution [19]. However, Andersen et al. [3] reported a fiber-type shift towards type 1 in vastus lateralis of DM1 patients, with type I fibers making up 64 % of the muscle in contrast to 38–47 % in healthy subjects [17]. It is possible that the increased level of ASI(−)RyR1 in DM1 patients [19] is due to the fiber-type shift in the muscle rather than aberrant splicing. Indeed, the high variability in fiber-type distribution seen in human subjects makes the strong correlation between fiber-type and ASI splice variant reported here all the more significant.

It is unclear from our data whether single muscle fibers contain both ASI splice variants or whether only one splice variant is present in the fiber. Muscle fibers that co-express different MyHC isoforms show contractile properties intermediate between those of fibers expressing only one or other of the MyHC isoforms [7, 21, 30, 31]. Similarly, individual slow twitch fibers express both isoforms of calsequestrin (CSQ1 and CSQ2; fast twitch only express CSQ1) which may facilitate optimal contractile function [21]. It may well be that individual fibers contain both ASI splice variants, with the ratio regulated to facilitate optimal EC coupling. In this case, the RyR1 channel would most likely be a heterotetramer containing various combinations of the two splice variants. Xu

Table 2 Densitometry of the ASI region PCR product with the corresponding fiber-type distribution

Muscle	Sex	Age	Type 1	Type 2A	Type 2X	Type 2	%ASI(+)	%ASI(-)
Gluteus medius	F	52	42.8	35.9	21.3	57.2	23.2	76.8
		76	59.7	24.2	16.1	40.3	47.2	52.8
		84	85.6	7.8	6.6	14.4	15.0	85.0
	M	72	78.2	15.3	6.5	21.8	30.4	69.6
Gluteus minimus	F	51	58.0	32.0	10.0	42.0	29.2	70.8
		52	81.8	13.3	4.9	18.2	24.9	75.1
		58	53.0	39.4	7.6	47.1	25.1	74.9
		61	58.2	26.7	15.1	41.8	31.3	68.7
		66	89.2	9.3	1.5	10.8	17.5	82.5
		70	44.1	31.5	24.4	55.9	22.4	77.6
		71	44.6	30.8	24.6	55.4	36.8	63.2
		74	67.9	22.3	9.9	32.1	41.9	58.1
		79	42.9	31.1	26.0	57.1	31.9	68.1
		82	58.1	31.8	10.1	41.9	20.9	79.1
		85	87.0	9.3	3.7	13.0	33.4	66.6
	M	45	50.0	36.3	13.7	50.0	42.5	57.5
		47	78.4	14.9	6.7	21.6	54.4	45.6
		52	41.8	34.3	23.9	58.2	33.1	66.9
		56	58.3	35.0	6.7	41.7	33.8	66.2
		59	49.5	33.6	16.9	50.5	20.7	79.3
		60	75.8	23.0	1.2	24.2	32.7	67.3
		61	52.9	38.6	8.5	47.1	51.8	48.2
		69	62.0	29.3	8.7	38.0	30.4	69.6
		70	45.3	37.8	16.9	54.7	37.7	62.3
		72	46.2	33.5	20.3	53.8	45.3	54.7
Vastus medialis	F	54	25.1	35.2	39.7	74.9	70.8	29.2
		56	29.9	43.0	27.1	70.1	57.5	42.5
		57	20.1	29.2	50.7	79.9	82.8	17.2
		62	25.0	46.6	28.4	75.0	61.3	38.7
		64	33.4	41.2	25.4	66.6	53.0	47.0
		64	32.0	47.0	21.0	68.0	54.0	46.0
		74	44.7	42.1	13.2	55.3	42.2	57.8
	M	59	31.0	40.8	28.2	69.0	57.6	42.4
		66	24.8	45.3	29.9	75.2	62.4	37.6
		69	27.7	33.6	38.7	72.3	78.3	21.7
		71	28.9	35.1	36.0	71.1	69.6	30.4
		73	35.0	40.8	24.2	65.0	59.0	41.0
		77	13.8	38.9	47.3	86.2	80.2	19.8

Values given for fiber type are averages of MyHC isoform as a percentage of the total MyHC. Values for type 2A and 2X are given separately (light grey shading) as well as together as type 2. Medium grey shading highlights muscle having high percentages of type 1 fibers and ASI(−)RyR1. Dark grey shading highlights muscle having high percentages of Type 2 fibers and ASI(+)RyR1

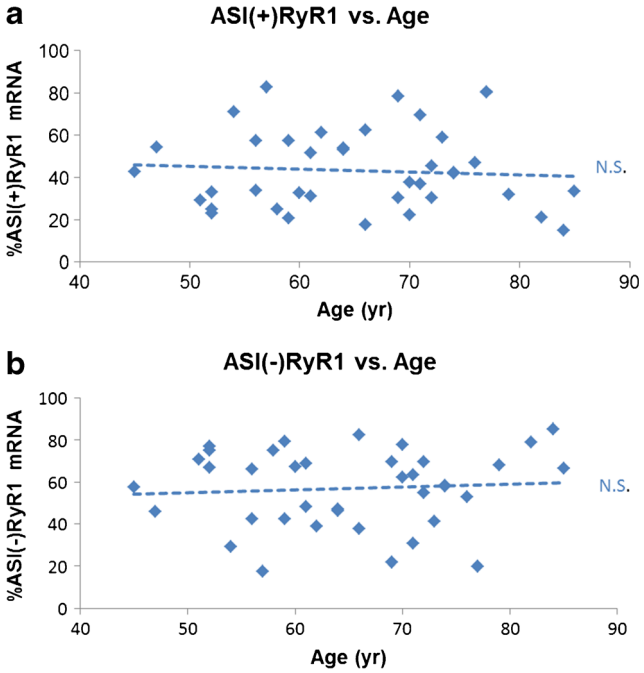

Fig. 4 The percentage of ASI(+)RyR1 and ASI(−)RyR1 transcripts plotted against the age of the respective donors. The data for all three muscles were combined in the graphs. **a** The percentage of ASI(+)RyR1 transcript with age. **b** The percentage of ASI(−)RyR1 transcript with age. *N.S.* no significant correlation

et al. [35] showed that the co-expression of WT RyR1 and a mutant RyR1 in HEK cells produced RyR1s that exhibited a range of phenotypes intermediate between the WT phenotype and the mutant [35]. If RyR1 contained both ASI(+) and

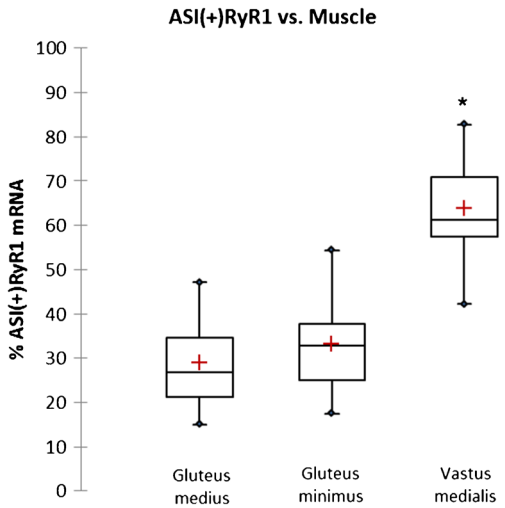

Fig. 5 Boxplots of the percentage of ASI(+)RyR1 transcript present in the different muscles from human donors. The *plus sign* indicates the mean percentage ASI(+)RyR1 transcript, the *top* and *bottom margins of the box* indicates the third and first quartile of the data set, respectively, and the *line in the middle of the box* indicates the median of the data set. The *whiskers* indicate the minimum and maximum point of the data set. *Significantly different from gluteus medius and gluteus minimus ($P<0.01$)

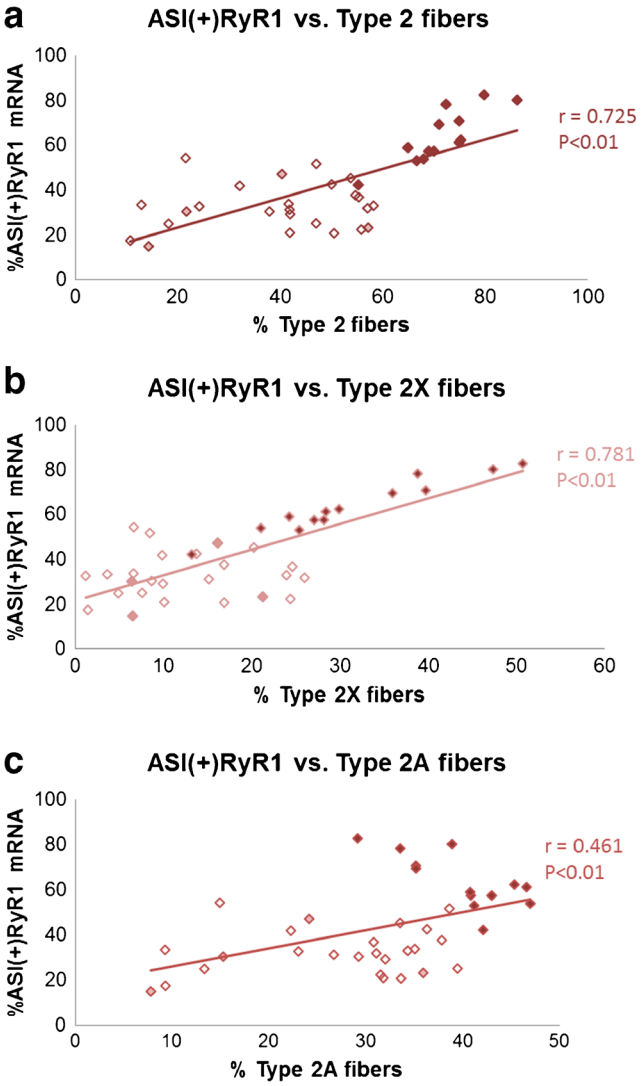

Fig. 6 The percentage of ASI(+)RyR1 transcript plotted against the fiber-type distribution of the muscle. The data for all three muscles were combined; however, data points from gluteus minimus is shown with *no fill*, gluteus medius with *light red fill*, and vastus medialis with *dark red fill*. **a** Correlation between the percentage of ASI(+)RyR1 transcript and percentage of type 2 fiber for all donors. **b** Correlation between the percentage of ASI(+)RyR1 transcript and perecentage of type 2X fiber for all the donors. **c** Correlation between percentage of ASI(+)RyR1 transcript and percentage of type 2A fiber for all the donors. *N.S.* no significant correlation, *r*=Pearson correlation coefficient

ASI(−) subunits, the channels would display a range of characteristics between those of homotetrameric ASI(+)RyR1 and ASI(−)RyR1 channels that could fine-tune the characteristics of EC coupling in individual fibers.

It is interesting to speculate on how the different ASI splice variants may contribute to EC coupling in fast and slow twitch skeletal muscle. Ca^{2+} release during EC coupling in RyR1-null myotubes transfected with ASI(−)RyR1 is almost double that in myotubes transfected with ASI(+)RyR1 [18]. A higher gain of EC coupling in the slow fibers may compensate for a number of structural factors that would otherwise tend to

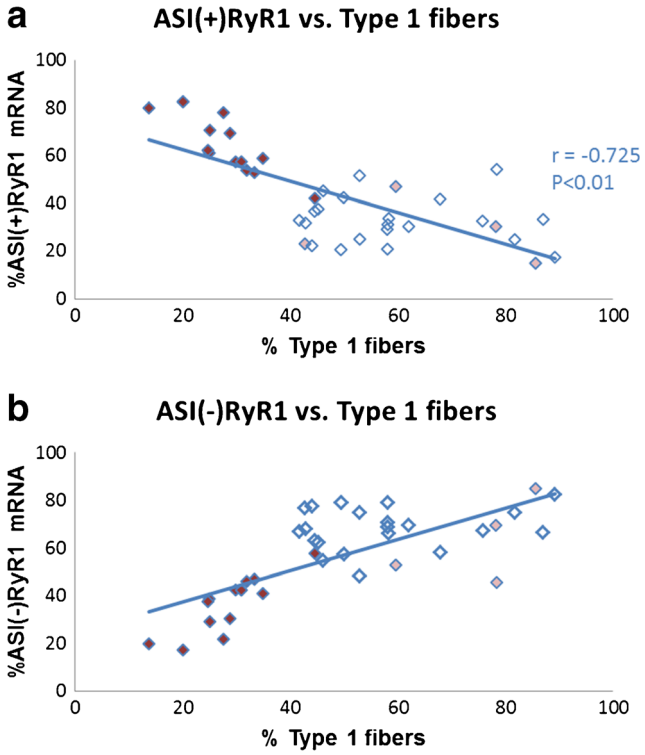

Fig. 7 The percentage of ASI(+)RyR1 and ASI(−)RyR1 transcripts plotted against the type 1fiber content in the muscle. The data for all three muscles were combined; however, data points from gluteus minimus is shown with *no fill*, gluteus medius with *light red fill*, and vastus medialis with *dark red fill*. **a** The percentage of ASI(+)RyR1 plotted against the percentage of type 1 fibers. **b** The percentage of ASI(-)RyR1 plotted against the percentage of type 1 fibers. *r*=Pearson correlation coefficient

reduce Ca^{2+} release. The number of SR/t-tubule junctions, the SR volume, and number of RyR1 feet per junction are all less in slow fibers than in faster fibers [13, 14]. In addition, the significantly smaller asymmetric charge movement indicates a lower density of DHPR voltage sensors [11]. However, the higher gain of EC coupling in the slow fibers would help to boost Ca^{2+} release from individual junctions to reported levels that are closer to those in faster fibers [4, 13].

The overall expression of RyR1 is significantly greater in vastus medialis compared to gluteus medius and gluteus minimus (Online resource 3). This is consistent with a predominantly fast twitch muscle type in vastus medialis as fast-twitch fibers generally have a larger and more developed SR and t-tubular network [13, 14, 32] and therefore have more RyR1. Also, there have been conflicting reports regarding the expression of RyR1 with age. A decrease in overall RyR1 levels (determined by 3[H]Ryanodine binding) with age has been reported in mixed and fast-twitch fibers of rats and mice [28, 29]. However, other ^{3}[H]Ryanodine binding and western blot studies report no change in RyR1 expression in fast- and slow-twitch muscle from aged rats [8, 20, 26]. We find that there is no correlation between age and RyR1 expression in the human muscles investigated in this study (Online resource 4).

We assume in the "Discussion" that the ASI splice variant messenger RNA (mRNA) levels translate into protein levels; however, ASI splice variant protein levels have not been evaluated in any studies thus for technical reasons. The splice variants differ in only five residues in >5000 and would not be separated on SDS-PAGE. In addition, the ASI region in the RyR1 protein is inaccessible to an antibody that detects a peptide corresponding to ASI(+) and surrounding residues [20]. This is likely because the ASI site is located in the closely packed helical domain 2 of RyR1 which is also partly occluded by the SPRY and P2 domains [36]. Thus, the isoforms would not be detected by immunoblot even if ASI(+)- and ASI(−)-specific antibodies with similar affinities for RyR1 could be developed. Western blotting remains a possibility if specific antibodies could be developed and if residual secondary structure did not prevent antibody recognition. Development of specific antibodies may be problematic as the regions surrounding the 5 ASI residues are conserved. Such development will be attempted in future studies but is beyond the scope of the current project. It is likely that the isoform protein levels will follow the mRNA levels because the mRNA levels are correlated with both the myopathy in DM1 [19] and with fiber-type differences in EC coupling ("Discussion" above). It is notable that levels of other muscle proteins closely follow mRNA levels [33].

Lack of fiber-type redistribution in aging human gluteus minimus, gluteus medius, and vastus medialis A change in myosin heavy chain isoform content could reflect either a change in fiber-type composition or a change in fiber size. Most studies investigating fiber cross-sectional area (usually in vastus lateralis) conclude that type 2 fibers become smaller with increasing age, whereas the type 1 fibers are much less affected [23, 27], while the numbers of each fiber type are similarly reduced. Thus, the cross-sectional area of the muscle occupied by type 2 fibers is significantly reduced with age because there are fewer fibers and they are smaller [23, 27]. In other words, because the age-related atrophy of muscle fibers is more severe in fast-twitch fibers, the proportion of muscle mass made up of slow-twitch fibers is increased, but the relative numbers of fast- and slow-twitch fibers do not change [12, 22–24].

As we did not examine single fiber dimensions, the results reflect the fraction of the whole muscle occupied by each fiber type. Gluteus medius and gluteus minimus were both dominated by type 1 fibers (61.5 and 59.5 %, respectively), whereas vastus medialis was dominated by type 2 (71.3 %). We found that type 1 fibers contribute to 28.7 % of vastus medialis mass. This is less than the percentage of type 1 fibers counted in myosin ATPase-stained cross sections of autopsy samples from six individuals aged 15 to 30: i.e. 43.7 % of fibers in

surface of vastus medialis or 61.5 % in deeper fibers [17]. The fact that type 2 fibers become smaller with age would exacerbate the difference between our results and others [2, 22, 24, 37]. It is difficult to speculate further on reasons for these differences given the very different techniques, the variability between individuals reported in all studies, and relatively small sample sizes.

We are unable to find reference to age-related changes in the three muscles used in this study. Most previous work in human muscle has been performed on vastus lateralis due to access for biopsy. In those studies, there was an increase in type 1 fiber content with age [23, 27], and we see a potential trend in that direction in gluteus medius. We find no significant correlation between fiber-type distribution and age in gluteus minimus and vastus medialis. However, as muscle was obtained from patients undergoing hip or knee replacements, it is possible that the muscle fiber types were already altered by inactivity and that this masked any changes due to age. It is likely that the variability between donors is also related to the genetic diversity within the human population, which would add to potential differences arising from gender, activity, and other factors.

Conclusions

The results presented here provide novel and compelling evidence that the expression of ASI RyR1 splice variants is fiber-type-dependent, in addition to being developmentally regulated. A fiber-type dependence of RyR1 isoforms has not previously been described in mammalian muscle, and its existence has potential implications for differences in Ca^{2+} dynamics during excitation contraction coupling in fast- and slow-twitch fiber types.

Acknowledgments The authors are grateful to Suzy Pace and to Joan Stivala for assistance with the collection of the human tissue and to NA Beard for helpful comment on the manuscript. The work was supported by grants from the National Health and Medical Research Council APP1020589 and APP1002589 as well as an Australian Postgraduate Award and a John Curtin School of Medical Research supplementary scholarship to HW.

References

1. Agbulut O, Noirez P, Beaumont F, Butler-Browne G (2003) Myosin heavy chain isoforms in postnatal muscle development of mice. Biol Cell 95:399–406
2. Andersen JL (2003) Muscle fibre type adaptation in the elderly human muscle. Scand J Med Sci Sports 13:40–47
3. Andersen G, Orngreen MC, Preisler N, Colding-Jorgensen E, Clausen T, Duno M, Jeppesen TD, Vissing J (2013) Muscle phenotype in patients with myotonic dystrophy type 1. Muscle Nerve 47:409–415. doi:10.1002/mus.23535
4. Baylor SM, Hollingworth S (2012) Intracellular calcium movements during excitation-contraction coupling in mammalian slow-twitch and fast-twitch muscle fibers. J Gen Physiol 139:261–272. doi:10.1085/jgp.201210773
5. Burkholder TJ, Fingado B, Baron S, Lieber RL (1994) Relationship between muscle fiber types and sizes and muscle architectural properties in the mouse hindlimb. J Morphol 221:177–190. doi:10.1002/jmor.1052210207
6. Cheng W, Altafaj X, Ronjat M, Coronado R (2005) Interaction between the dihydropyridine receptor Ca^{2+} channel beta-subunit and ryanodine receptor type 1 strengthens excitation-contraction coupling. Proc Natl Acad Sci U S A 102:19225–19230. doi:10.1073/pnas.0504334102
7. Cvetko E, Karen P, Erzen I (2012) Myosin heavy chain composition of the human sternocleidomastoid muscle. Ann Anat 194:467–472. doi:10.1016/j.aanat.2012.05.001
8. Damiani E, Larsson L, Margreth A (1996) Age-related abnormalities in regulation of the ryanodine receptor in rat fast-twitch muscle. Cell Calcium 19:15–27
9. Dedkov EI, Kostrominova TY, Borisov AB, Carlson BM (2001) Reparative myogenesis in long-term denervated skeletal muscles of adult rats results in a reduction of the satellite cell population. Anat Rec 263:139–154. doi:10.1002/ar.1087
10. Deschenes MR (2011) Motor unit and neuromuscular junction remodeling with aging. Curr Aging Sci 4:209–220
11. Dulhunty AF, Gage PW (1983) Asymmetrical charge movement in slow- and fast-twitch mammalian muscle fibres in normal and paraplegic rats. J Physiol 341:213–231
12. Essen-Gustavsson B, Borges O (1986) Histochemical and metabolic characteristics of human skeletal muscle in relation to age. Acta Physiol Scand 126:107–114. doi:10.1111/j.1748-1716.1986.tb07793.x
13. Franzini-Armstrong C, Ferguson DG, Champ C (1988) Discrimination between fast- and slow-twitch fibres of guinea pig skeletal muscle using the relative surface density of junctional transverse tubule membrane. J Muscle Res Cell Motil 9:403–414
14. Franzini-Armstrong C, Protasi F, Ramesh V (1999) Shape, size, and distribution of Ca^{2+} release units and couplons in skeletal and cardiac muscles. Biophys J 77:1528–1539. doi:10.1016/S0006-3495(99)77000-1
15. Futatsugi A, Kuwajima G, Mikoshiba K (1995) Tissue-specific and developmentally regulated alternative splicing in mouse skeletal muscle ryanodine receptor mRNA. Biochem J 305(Pt 2):373–378
16. Harper PS (2001) Myotonic dystrophy. 3rd ed. / with a chapter on molecular and cell biology by J. David Brook and Emma Newman. edn. W.B. Saunders, London
17. Johnson MA, Polgar J, Weightman D, Appleton D (1973) Data on the distribution of fibre types in thirty-six human muscles. An autopsy study. J Neurol Sci 18:111–129
18. Kimura T, Lueck JD, Harvey PJ, Pace SM, Ikemoto N, Casarotto MG, Dirksen RT, Dulhunty AF (2009) Alternative splicing of RyR1 alters the efficacy of skeletal EC coupling. Cell Calcium 45:264–274. doi:10.1016/j.ceca.2008.11.005
19. Kimura T, Nakamori M, Lueck JD, Pouliquin P, Aoike F, Fujimura H, Dirksen RT, Takahashi MP, Dulhunty AF, Sakoda S (2005) Altered mRNA splicing of the skeletal muscle ryanodine receptor and sarcoplasmic/endoplasmic reticulum Ca^{2+}-ATPase in myotonic dystrophy type 1. Hum Mol Genet 14:2189–2200. doi:10.1093/hmg/ddi223
20. Kimura T, Pace SM, Wei L, Beard NA, Dirksen RT, Dulhunty AF (2007) A variably spliced region in the type 1 ryanodine receptor may participate in an inter-domain interaction. Biochem J 401:317–324. doi:10.1042/BJ20060686
21. Lamboley CR, Murphy RM, McKenna MJ, Lamb GD (2013) Endogenous and maximal sarcoplasmic reticulum calcium content and calsequestrin expression in type I and type II human skeletal

muscle fibres. J Physiol 591:6053–6068. doi:10.1113/jphysiol.2013.265900
22. Larsson L, Sjodin B, Karlsson J (1978) Histochemical and biochemical changes in human skeletal muscle with age in sedentary males, age 22–65 years. Acta Physiol Scand 103:31–39. doi:10.1111/j.1748-1716.1978.tb06187.x
23. Lexell J (1995) Human aging, muscle mass, and fiber type composition. J Gerontol A Biol Sci Med Sci 50 Spec No:11–16
24. Lexell J, Taylor CC, Sjostrom M (1988) What is the cause of the ageing atrophy? Total number, size and proportion of different fiber types studied in whole vastus lateralis muscle from 15- to 83-year-old men. J Neurol Sci 84:275–294
25. Mizunoya W, Wakamatsu J, Tatsumi R, Ikeuchi Y (2008) Protocol for high-resolution separation of rodent myosin heavy chain isoforms in a mini-gel electrophoresis system. Anal Biochem 377:111–113. doi:10.1016/j.ab.2008.02.021
26. O'Connell K, Gannon J, Doran P, Ohlendieck K (2008) Reduced expression of sarcalumenin and related Ca2+—regulatory proteins in aged rat skeletal muscle. Exp Gerontol 43:958–961. doi:10.1016/j.exger.2008.07.006
27. Porter MM, Vandervoort AA, Lexell J (1995) Aging of human muscle: structure, function and adaptability. Scand J Med Sci Sports 5:129–142
28. Renganathan M, Messi ML, Delbono O (1997) Dihydropyridine receptor-ryanodine receptor uncoupling in aged skeletal muscle. J Membr Biol 157:247–253
29. Renganathan M, Messi ML, Delbono O (1998) Overexpression of IGF-1 exclusively in skeletal muscle prevents age-related decline in the number of dihydropyridine receptors. J Biol Chem 273:28845–28851
30. Rhee HS, Lucas CA, Hoh JF (2004) Fiber types in rat laryngeal muscles and their transformations after denervation and reinnervation. J Histochem Cytochem 52:581–590
31. Rivero JL, Talmadge RJ, Edgerton VR (1998) Fibre size and metabolic properties of myosin heavy chain-based fibre types in rat skeletal muscle. J Muscle Res Cell Motil 19:733–742
32. Schiaffino S, Reggiani C (2011) Fiber types in mammalian skeletal muscles. Physiol Rev 91:1447–1531. doi:10.1152/physrev.00031.2010
33. Soukup T, Diallo M (2015) Proportions of myosin heavy chain mRNAs, protein isoforms and fiber types in the slow and fast skeletal muscles are maintained after alterations of thyroid status in rats. Physiol Res 64:111–118
34. Talmadge RJ, Roy RR (1993) Electrophoretic separation of rat skeletal muscle myosin heavy-chain isoforms. J Appl Physiol 75:2337–2340
35. Xu L, Wang Y, Yamaguchi N, Pasek DA, Meissner G (2008) Single channel properties of heterotetrameric mutant RyR1 ion channels linked to core myopathies. J Biol Chem 283:6321–6329. doi:10.1074/jbc.M707353200
36. Yan Z, Bai XC, Yan C, Wu J, Li Z, Xie T, Peng W, Yin CC, Li X, Scheres SH, Shi Y, Yan N (2015) Structure of the rabbit ryanodine receptor RyR1 at near-atomic resolution. Nature 517:50–55. doi:10.1038/nature14063
37. Yu F, Hedstrom M, Cristea A, Dalen N, Larsson L (2007) Effects of ageing and gender on contractile properties in human skeletal muscle and single fibres. Acta Physiol (Oxf) 190:229–241. doi:10.1111/j.1748-1716.2007.01699.x
38. Zorzato F, Sacchetto R, Margreth A (1994) Identification of two ryanodine receptor transcripts in neonatal, slow-, and fast-twitch rabbit skeletal muscles. Biochem Biophys Res Commun 203:1725–1730. doi:10.1006/bbrc.1994.2385